CYTOLOGICAL STUDIES OF ORGANOTYPIC CULTURES OF RAT DORSAL ROOT GANGLIA FOLLOWING X-IRRADIATION IN VITRO

II. Changes in Schwann Cells, Myelin Sheaths, and Nerve Fibers

EDMUND B. MASUROVSKY, MARY BARTLETT BUNGE, and RICHARD P. BUNGE

From the Department of Anatomy, Columbia University College of Physicians and Surgeons, New York

ABSTRACT

Under suitable conditions rat dorsal root ganglia differentiate and myelinate in culture, providing an organotypic model of the ganglion (8). Mature cultures of this type were irradiated with a 40 kR dose of 184 kvp X-rays and, after daily observation in the living state, were fixed for light and electron microscopy. Within 24 hr after irradiation, numerous Schwann cells investing unmyelinated axons acutely degenerate. The axons thus denuded display little change. Conversely, few ultrastructural changes develop in Schwann cells investing myelinated axons until after the 4th day. During the 4–14 day period, these Schwann cells and their related myelin sheaths undergo progressive deterioration. Associated axons decrease in diameter but are usually maintained. Myelin deterioration begins as a nodal lengthening and then progresses along two different routes. In intact Schwann cells, fragmentation of myelin begins in a pattern reminiscent of Wallerian degeneration, but its slow breakdown thereafter suggests metabolic disturbances in these Schwann cells. The second pattern of myelin deterioration, occurring after complete degeneration of the related Schwann cell, involves unusual configurational changes in the myelin lamellae. Atypical repeating periods are formed by systematic splitting of lamellae at each major dense line with further splitting at the intraperiod line (Type I) or by splitting in the region of every other intraperiod line (Type II); some sheaths display a compact, wavy, inner zone and an abnormally widened lamellar spacing peripherally (Type III). Extensive blebbing of myelin remnants characterizes the final stages of this extracellular myelin degradation. These observations provide the first description of ultrastructural changes produced by ionizing radiation in nerve fascicles in vitro.

INTRODUCTION

The first demonstration of morphological as well as functional changes produced by ionizing radiation in nerve fiber bundles of the peripheral nervous system was reported by Redfield et al. (1) in 1922. They noted that myelin sheath deterioration accompanied the loss of impulse conduction in frog peripheral nerve after exposure to radium emissions. Leboucq (2) reported similar degenera-

tive changes in peripheral nerve elements of newborn rats which had received 4 kR of roentgen radiation (X-rays). A few years later (1936) Mogil'nitskiy et al. (3) noted proliferation of Schwann cells, histiocytes, and interstitial cells 10 days following exposure to 0.9 kR of X-rays. When the dose was increased to 1.5–1.8 kR, zones of demyelination, axonal distention, and infiltration of Schwann cells also occurred. In contrast, Janzen and Warren (4) reported that they were unable to detect any histological or functional change in rat sciatic nerve which had been subjected to a 6–10 kR dose of X-rays. Doses of 75–100 kR radium γ-rays, having a relative biological effectiveness similar to X-rays, did abolish impulse conduction and caused severe degeneration of axons and myelin sheaths. These changes were accompanied by a significant increase in the Schwann cell and lymphocyte populations. The disparate results obtained by these early investigators may have been due to variation in the species studied, differences in types of radiation and dose rates employed, or complications introduced by radiation damage to the differing vasculature of the nerves studied.

More recent studies have begun to provide a more detailed picture of the histological changes occurring after irradiation of peripheral nerve in vivo. Isomäki et al. (5) noted acute Schwann cell degeneration as well as axon changes following kilorad doses of α-particle radiation of the nerves in frog skin, and they advanced the suggestion that Schwann cells related to unmyelinated fibers might be more sensitive to radiation damage than Schwann cells related to myelin sheaths. Bergström (6) reported that paresis accompanied myelin degeneration, axonal distortion, Schwann cell proliferation, and extensive pathological vascular changes following the absorption, in rat sciatic nerve, of 20–40 krad of 185-Mev protons. He attempted but was unable to ascertain, from this light microscopic investigation, which degenerative changes had resulted from "direct" effects of the high energy protons on the nerve fascicles and which were secondary effects attributable to radiation damage to the associated vascular supply. Andres (7) employed the same 185-Mev protons at similar doses in an electron microscope study of the cytological changes produced in rat peripheral nervous tissue irradiated in vivo. Concentrating on observations obtained 6–18 days after irradiation, Andres described the sequential pathological changes occurring in axons, Schwann cells, and myelin sheaths. He believed that the changes he observed in axonal mitochondria and neurofilaments reflected changes in the neuronal soma and were independent of lesions in the related Schwann cells. The earliest myelin changes occurred at the node of Ranvier and subsequently progressed along the internode, the myelin becoming a series of balls to be digested within "phagosomes" (either in the Schwann cell cytoplasm or, after transfer, in phagocyte cytoplasm). Myelin degeneration often occurred in the company of an axon which had been pushed to one side of the endoneurial tube. Vascular tissue also suffered extensive damage and, therefore, Andres, like Bergström before him, was unable to determine which effects he observed were the result of primary radiation damage to the axons, myelin sheaths, and Schwann cells per se and which were secondary manifestations of the altered vascular supply to the irradiated nerve. His electron microscopic observations of tissue in situ serve as a valuable point of comparison for this in vitro study.

The present paper reports results of experiments designed to help resolve this question of "primary" or "direct" versus "secondary" or "indirect" effects of ionizing radiation (as defined in a previous paper, 10) on mammalian peripheral nerve. The histological fidelity of nerve fascicles in culture (8) permits these to serve as a model for the in vivo peripheral nerve fiber bundle without the vascular system component. A companion paper (10) deals with postirradiation changes in the neurons and supporting cells in the explant region of these same cultures.

MATERIALS AND METHODS

A detailed description of the techniques utilized in culturing the rat dorsal root ganglia together with the fixation, embedding, staining, and microscopic protocols appear elsewhere (8, 9). The cultures, prepared from explants taken from 18–20-day rat fetuses, were irradiated after 8–12 wk in vitro. All were considered fully differentiated, i.e., mature, by criteria discussed in reference 8. They received 40 kR of 184 kvp X-rays at a dose rate of 1 kR per min. The irradiation procedure employed is fully described in the preceding paper (10). These cultures, along with nonirradiated controls, were observed daily in the living state. At intervals of 1, 4, 8, and 14 days after irradiation, 4 or more cultures were prepared for electron microscopy; similar cultures

were fixed and stained for light microscopic examination.

OBSERVATIONS

Nerve fibers in long-term dorsal root ganglion cultures are gathered into fascicles containing myelinated and unmyelinated axons. Usually, several unmyelinated axons are invested by a single Schwann cell. Other Schwann cells ensheath singly occurring axons with compacted myelin, each internode being associated with a single fusiform Schwann cell nucleus. A basement membrane coats the outer surface of the Schwann cell, and collagen fibrils are scattered throughout the intrafascicular space within a perineurial mantel. A detailed light and electron microscopic description of these various elements may be found in the first paper of this series (8).

1 Day after Irradiation

The most striking observation during the first 24 hr following irradiation is that many Schwann cells investing unmyelinated axons appear acutely degenerated whereas the Schwann cells containing myelinated axons display relatively few morphological changes. This dichotomy in response to radiation exposure among the Schwann cell

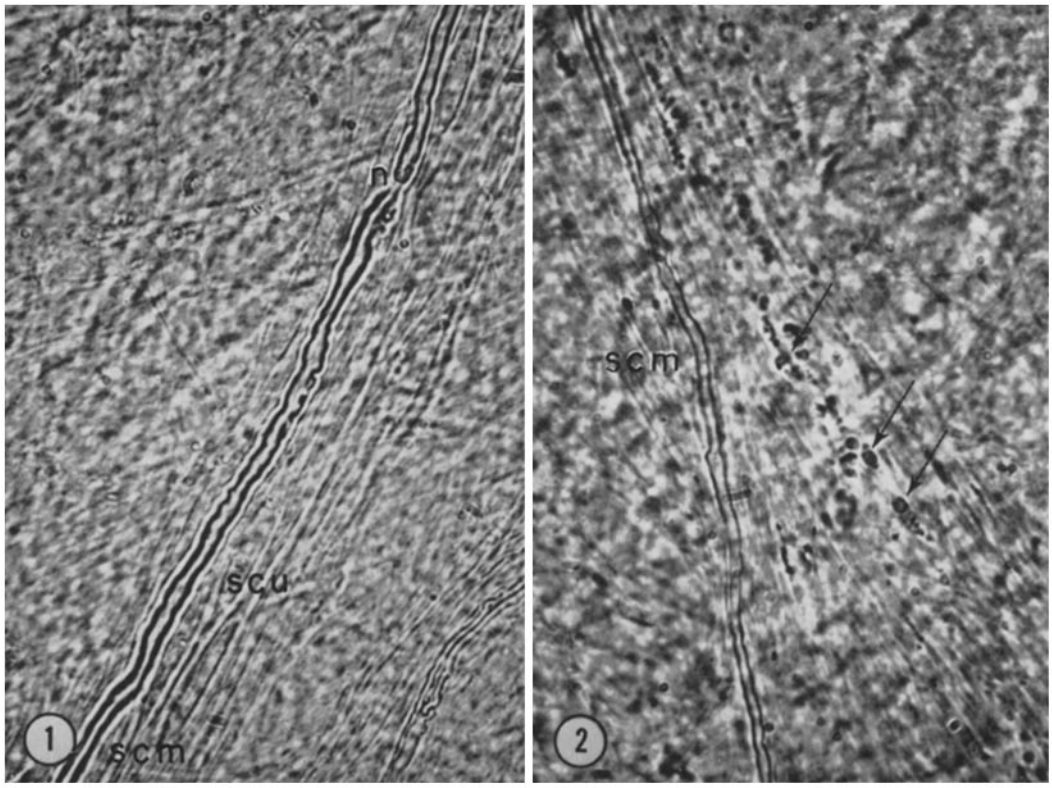

FIGURE 1 This figure is representative of fiber bundle regions in control rat dorsal root ganglion cultures as seen in the living state. A typical myelinated fiber with normal-appearing sheath and associated Schwann cell nucleus (*scm*) and a node of Ranvier (*n*) may be seen in this field. Characteristc fusiform cells of Schwann (*scu*) appear among the unmyelinated fibers of this fascicle. Connective tissue elements form a textured background. × 690.

FIGURE 2 A similar fiber bundle region as seen in the living state *24 hrs following X-irradiation.* The myelin sheath and associated Schwann cell nucleus (*scm*) appear generally normal whereas cellular debris (arrows) is evident among the unmyelinated fibers. Such cell remnants are seen in the electron microscope to result from degenerating Schwann cells. × 690.

population is dramatically seen *in the living cultures*. The nerve fiber bundles, previously filled with fusiform Schwann cell nuclei related to myelinated or unmyelinated fibers (Fig. 1), now are sites of fragmented and granular cellular debris (Fig. 2). This debris is prominent in areas of unmyelinated fibers. Myelin sheaths and their associated Schwann cells and paranodal regions appear normal (Fig. 2). These pathological changes contrast with the generally normal appearance of

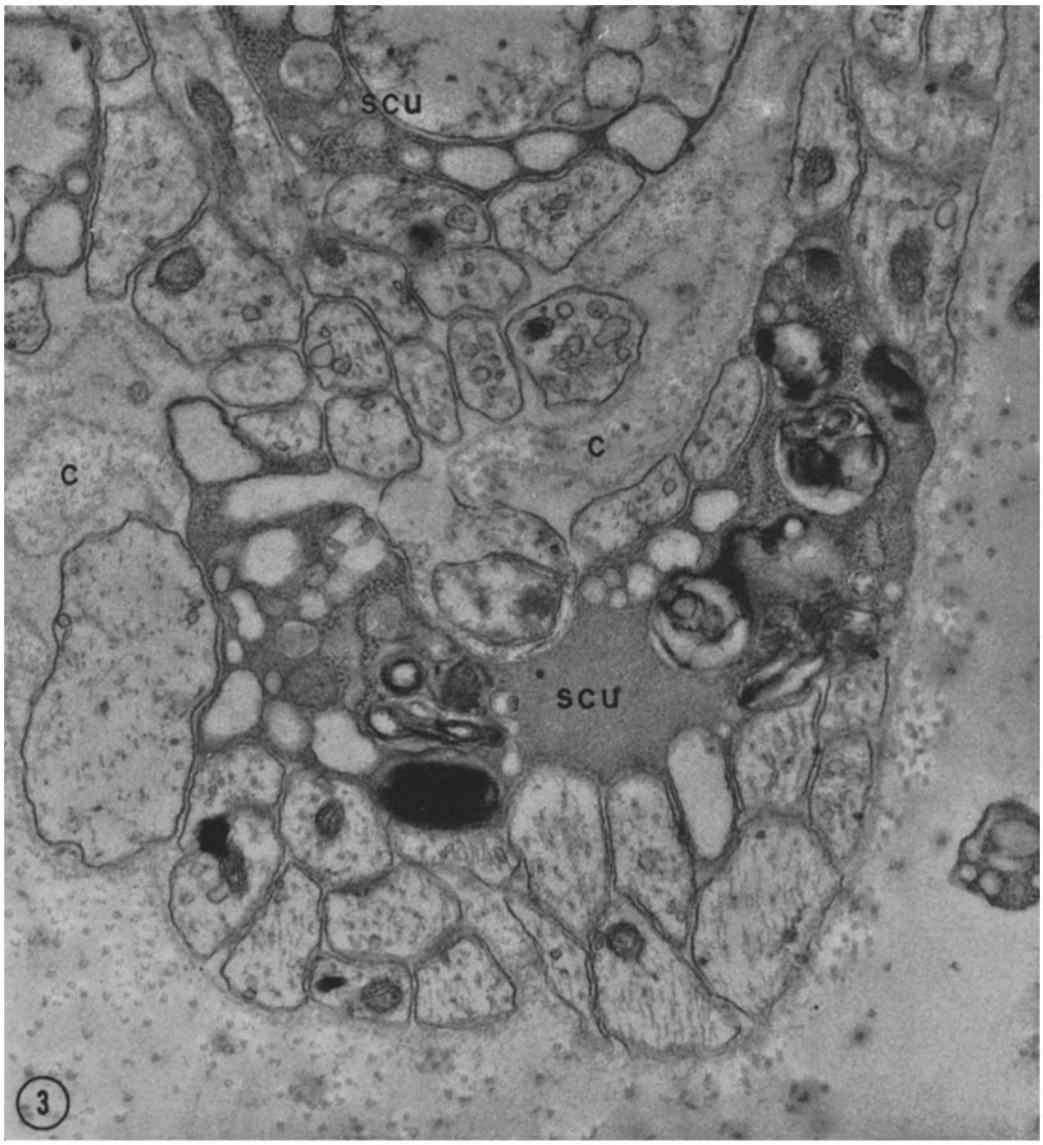

FIGURE 3 This electron micrograph shows a region of unmyelinated nerve fibers *24 hr after irradiation*. The Schwann cells (*scu*) associated with these fibers are undergoing acute degeneration; they appear abnormally dense and contain pathological membranous, vacuolar bodies. Though some axons have been divested of Schwann cell cytoplasm, they remain within the basement membrane left by these cells and appear generally normal in morphology. Collagen fibrils (*c*), in various planes of section, are distributed throughout the intrafascicular space. × 30,000.

the neurons at this stage, but coincide with the acute degeneration in many of the neuron-ensheathing satellite cells. The temporal relationship of this early satellite cell necrosis (described in the previous paper, 10) and the early Schwann cell deterioration mentioned above may suggest some metabolic kinship between these two cell types. The organization of the perineurium appears unchanged.

The fact that the degenerating cells in nerve fascicles observed in the light microscope are indeed acutely necrotic Schwann cells related to unmyelinated axons can be definitely shown *in the electron microscope* (Fig. 3). Degenerating Schwann cell cytoplasm may be abnormally dense and vacuolar. Following Schwann cell loss, the denuded unmyelinated axons continue to appear relatively normal morphologically and remain encased within the basement membrane which previously coated the Schwann cell. The structural integrity exhibited by axons following exposure sufficient to damage other cellular elements has been previously noted and commented upon by other investigators studying both central and peripheral nervous tissue (7, 11–13). Basement membranes have been found to be relatively stable structures following irradiation in vivo (7) and Wallerian degeneration (14–16, among others). External to the basement membrane, collagen fibrils are distributed as usual throughout the intrafascicular space. Electron microscopic observations confirm the initial impression that the myelin-related Schwann cells and myelin sheaths, including nodal areas, appear essentially unaltered in structure at this time.

4 Days after Irradiation

Light microscopic observations at this interval indicate that, as at 1 day, the fascicles contain many remnants of acutely degenerated cells; these remnants become less prominent with time. The first sign of myelin alteration appears at this time as a shortening of the internode with consequent nodal lengthening. Nodal alterations, as the initial event in myelin damage, characterize several types of demyelination which will be discussed with the 8-day observations.

The *electron microscope* indicates that, despite these early nodal alterations, the structure of internodal myelin is little altered at this stage (Fig. 4). Only minor changes are noted in the myelin-related Schwann cells. Unmyelinated fibers are often completely denuded of Schwann cells by this time, although associated remnants of Schwann cell cytoplasm may be present (Fig. 4). Neither at this interval nor at any of the others studied are there any indications of the Schwann cell proliferation so frequently observed following irradiation in vivo (see Introduction).

8 Days after Irradiation

Between the 4th and 8th day following irradiation, myelin abnormalities become conspicuous *in the living cultures.* The radiation response of the Schwann cell–myelin unit varies and may be categorized as follows: (*a*) Some Schwann cells related to myelinated axons remain essentially unaltered morphologically throughout the 14 day observation period; these are a small minority. (*b*) In a substantial number of myelin segments, deterioration of the sheath occurs in necrotic Schwann cells. In this situation, the tubular form of the myelin is generally preserved though the sheath is split, swollen, or distorted. This type of myelin breakdown is characterized by an intact axon surrounded by greatly altered sheath material devoid of viable Schwann cytoplasm. It is most marked 14 days after irradiation and will be described in detail in that section. (*c*) Many myelin sheaths undergo breakdown from the normal tubular form to a series of round or oval fragments within the cytoplasm of the associated Schwann cells in which partial breakdown of the contained myelin debris occurs. In this way, the process resembles the type of myelin breakdown seen in Wallerian degeneration.

The complex interaction between the Schwann cell and its myelin sheath during this third type of change must be analyzed at both the light and electron microscope levels. Daily examination of the living culture indicates that the remnants of an internode of myelin are taken up by the Schwann cell which had formed that internode. In contrast to Wallerian degeneration, this process occurs in tandem with internodes undergoing either no change or other types of degeneration, indicating that the axon is intact. *In the electron microscope,* the irradiated Schwann cell associated with this type of myelin breakdown exhibits a variety of irregular, ellipsoidal myelin fragments within cytoplasm engorged with pathological vesiculated and granular bodies (Fig. 5). These bodies and the wealth of vesicles present appear to be derived, at least in part, from the demise of various cyto-

FIGURE 4 In this electron micrograph of a fiber bundle *4 days following irradiation,* most unmyelinated axons are completely denuded of Schwann cell processes but still reside within basement membrane. Myelinated axons, on the other hand, remain within intact, somewhat altered Schwann cells (*scm*), and their myelin sheaths do not differ significantly from the normal. × 30,000.

plasmic organelles. Typical granular endoplasmic reticulum cisternae and free ribosomes are greatly reduced in amount, filaments are sparse, and identifiable Golgi complexes are no longer found. This is in contrast to the appearance of Schwann cells during Wallerian degeneration when they are hypertrophied and show, in particular, an increase in the number of ribosomes (15, 18, 19). This aspect of the Schwann cell response to irradiation is considered in more detail in the Discussion. Lipid droplets and granular lysosome-like bodies are present in the irradiated myelin-ingesting

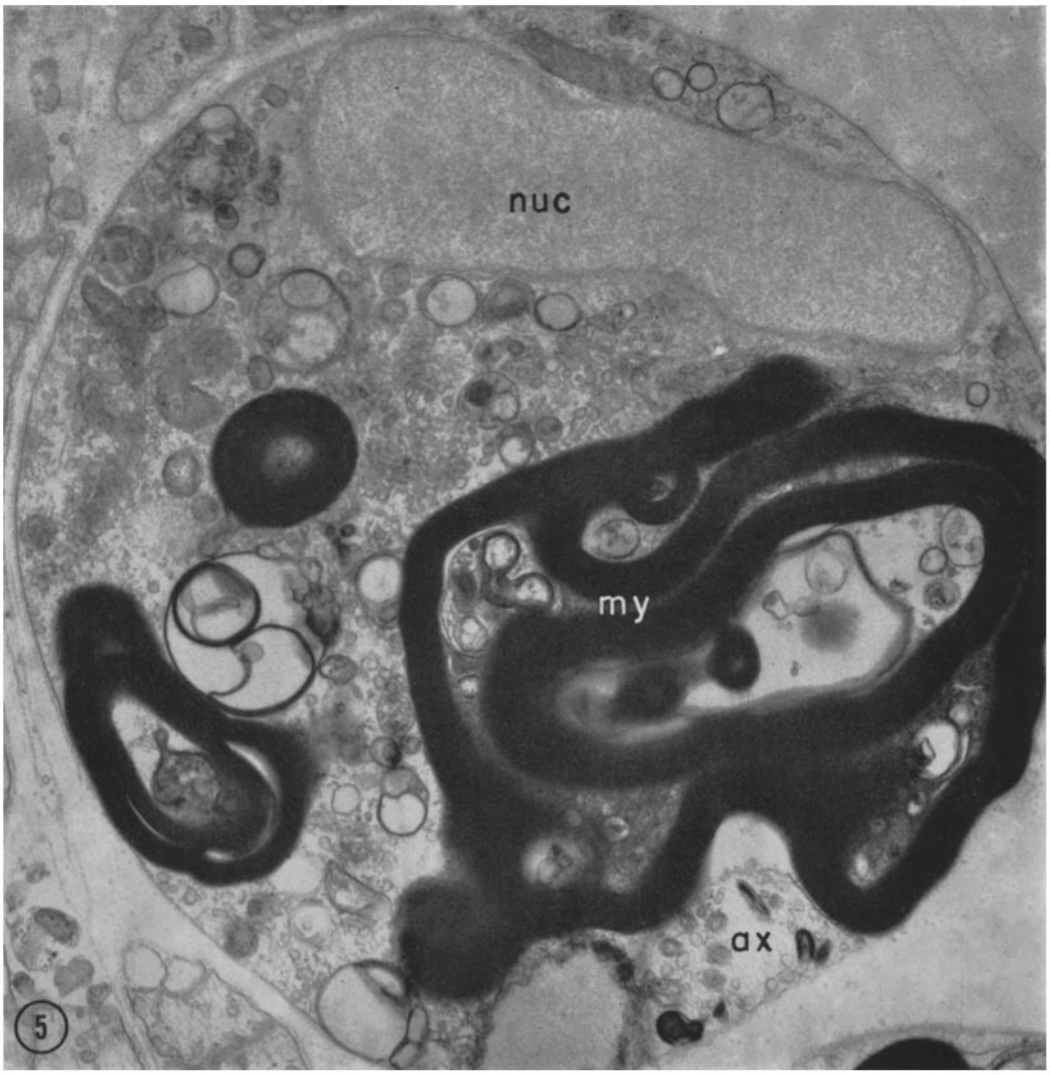

FIGURE 5 This abnormal-appearing Schwann cell contains myelin debris (*my*) and a variety of vesicular and vacuolar cytoplasmic structures *8 days following irradiation.* A portion of the nucleus (*nuc*) is present. An axon appears at *ax*. × 13,000.

Schwann cells. In these Schwann cells, an unusual form of myelin breakdown is sometimes observed (Figs. 6 and 7). Instead of myelin ovoids being enclosed in the usual digestion vacuoles (20), unraveling lamellae appear to invaginate the Schwann cell cytoplasm. Various lengths of myelin-containing vesicles are formed from these structures. These vesicles may be the site of myelin degradation or they may serve to enclose and transfer small myelin fragments to larger vacuoles for breakdown.

Lengthening of the node of Ranvier is noted consistently in irradiated cultures at this time. This appears to affect almost all nodes regardless of the type of terminal degeneration the myelin may undergo. Comparison of control and irradiated cultures by bright-field and polarizing microscopy (Figs. 8 and 9) reveals the greatly lengthened nodal distance of irradiated fibers. An electron microscope view of a region bordering a lengthened node of Ranvier is presented in Fig. 10. The terminating myelin loops as well as the normally interlacing

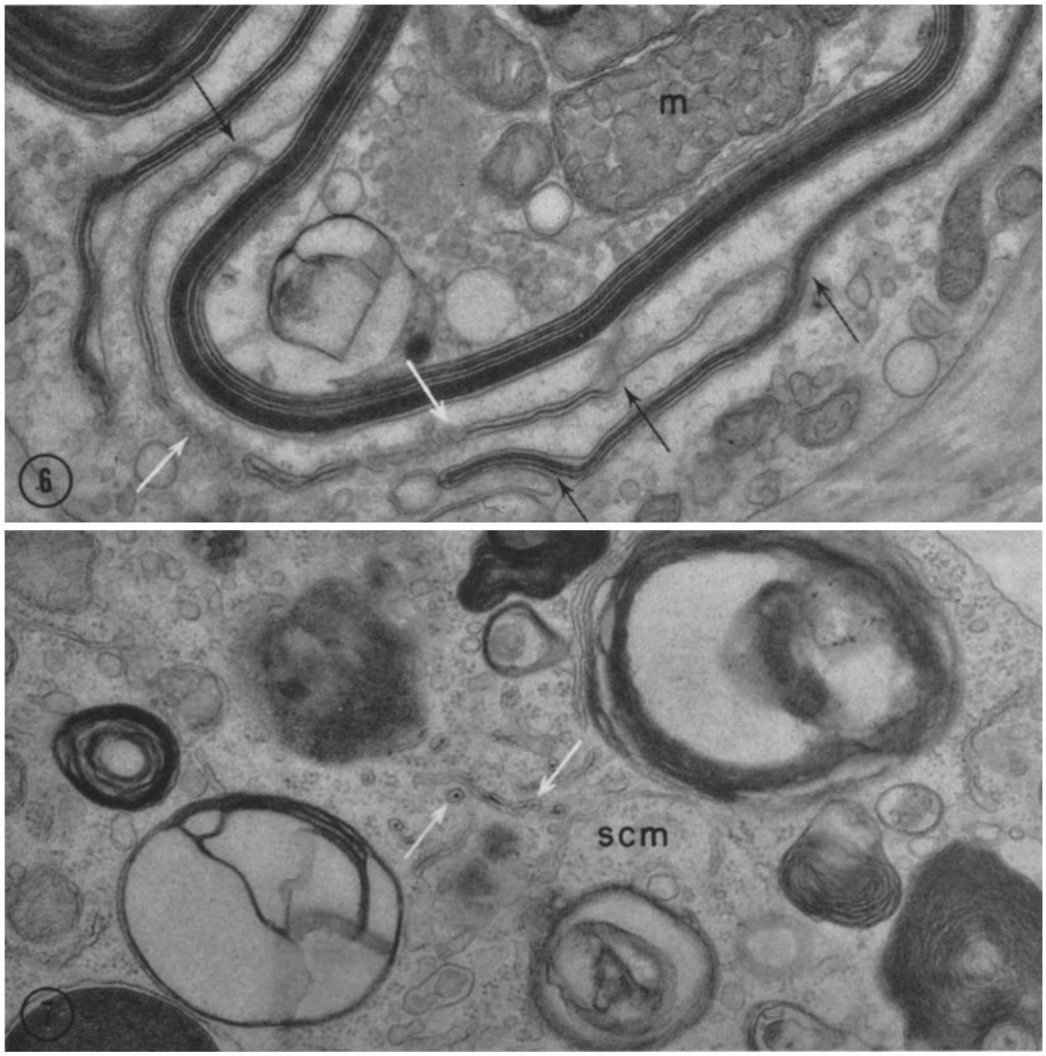

FIGURE 6 This electron micrograph of an abnormal Schwann cell displays a type of myelin breakdown heretofore not reported in the PNS. Unraveling lamellae are invaginated into the Schwann cell cytoplasm (black arrows) where they are pinched off into vesicular elements of various lengths (white arrows). Abnormal mitochondrion at *m*. *8 days after irradiation*. × 38,000.

FIGURE 7 This Schwann cell (*scm*) contains segments of membrane-bounded material with a dense core (arrows) which may represent some of the pinched-off myelin elements described in Fig. 6. *8 days after irradiation*. × 38,000.

Schwann cell projections at the nodal junction have ruptured and begun to deteriorate. Schwann cell and myelin breakdown is in evidence at adjacent sites along this paranodal segment. Andres (7) reported that myelin degeneration near the node of Ranvier was one of the first signs of myelin deterioration in rat dorsal root ganglia after irradiation in vivo. The node-supporting functions of the Schwann cell appear, on the basis of both in vivo and in vitro studies, to be quite radiosensitive. Further evidence for the sensitivity of the nodal region to noxious conditions is presented by Webster et al. in vivo (21) and Peterson and Murray in vitro (17); both

noted paranodal alterations as the earliest myelin change in experimental diphtheritic neuritis.

Despite the major changes in myelin and Schwann cells at this 8-day postirradiation interval most axons are retained, for, up to this point, there has been little neuronal loss (10). Many axons, whether unmyelinated or previously myelinated, display minimal morphological alterations; some appear to have decreased in diameter. Pathological changes which have been noted in axons are (*a*) unusual glycogen-containing membranous arrays (Fig. 11) closely resembling those described by Steiner et al. (22) in liver cells of ethionine-intoxicated rats and, more frequently, (*b*) abnormal accumulations of mitochondria with associated glycogen-like particles. The identification of these particles as glycogen is discussed in the other papers of this series (8, 10). The appearance of glycogen granules in axons following irradiation has been reported in frog sympathetic nerve by Pick (23). He has discussed the possible significance of this finding.

14 Days after Irradiation

Nodal lengthening, axonal alterations, and Schwann cell deterioration are accompanied by further changes in the associated myelin sheaths two weeks after irradiation. These changes may be observed at the light microscopic level *in living cultures* (Figs. 12 and 13). Next to relatively normal-looking myelinated fibers are sheaths undergoing Wallerian-like degeneration or considerable distortion and swelling. Intact though abnormally distorted axons may be seen within sheaths which are undergoing swelling (arrow, Fig. 13). Often Schwann cell nuclei cannot be found in relation to these segments. As mentioned above, in this type of breakdown the general tubular form of the myelin sheath is retained despite the advanced state of degeneration in the accompanying Schwann cell.

In this type of "swelling" degeneration, unusual reorderings in the periodicity and dimensions of the myelin lamellae are observed by *electron microscopy*. A sequence of such myelin splitting and reordering is illustrated in Fig. 14. The normal-appearing inner sheath lamellae end abruptly by splitting at the major dense line. From this point, irregular 120–150-A elements, apparently composed of the intraperiod line sandwiched between two less dense layers, spiral outward. These irregular lamellar structures form a "period" of 240–260 A. In the more peripheral regions of the sheath, further splitting occurs at the intraperiod line forming a subperiod of ~150 A. This pattern of myelin change is designated Type I and is diagrammed in Fig. 18. The Schwann cell cytoplasm has completely degenerated around the outside and inside of the sheath as has the inner mesaxon. Thus, the electron microscope establishes that this unusual pattern of myelin breakdown occurs where the associated Schwann cell has completely degenerated. The axon, on the other hand, exhibits no remarkable ultrastructural change. A more advanced form of Type I myelin sheath breakdown is shown in Fig. 15. Considerable splitting has occurred at the intraperiod line, forming 60–70 A lamellar elements. Note the bleblike myelin remnants internal to the sheath around the deformed axon and external to the sheath, plus the small neurite-like processes within the confines of the residual basement membrane.

Another type of myelin reordering (Type II) is depicted in Fig. 16. It is distinguished by broad regions of abnormally spaced paired lamellar elements notable for their riblike regularity. The paired unit measures 240 A, and the distance from the middle of one unit to another is about 300 A (Fig. 18). It appears that these units are formed by splitting in the area of every other intraperiod line. This pattern resembles the separations of lamellar units along alternating intraperiod lines in rat optic nerve immersed in hypotonic solutions, reported by Finean and Burge (24). In Type II splitting in the irradiated cultures, irregular fissures are produced by distention and rupturing within the paired unit. Still another pattern of abnormal myelin structuring (Type III) is shown in Fig. 17. It is noteworthy for its wavy inner sheath lamellae which appear to open out into a ~210–240 A spacing. Splitting appears to occur in regions between major dense lines (Fig. 18). Such myelin configurations are observed only in segments in which the associated Schwann cells are necrotic.

All three types of myelin deterioration may share a common terminal route of degeneration characterized by the formation of striking, variegated, alveolar patterns (Fig. 19). Vacuolar or tubular structures are formed at the ends of fractured myelin elements; they are usually bounded by profiles of varying thickness and density. Myriads of these blebs come to fill the volume delineated by the residual Schwann cell basement membrane.

These distinctive forms of myelin degradation following irradiation will be related to previously observed patterns of myelin breakdown and to the condition of the associated Schwann cell in the discussion below.

Neurite-like processes may be seen within the basement membrane in Figs. 15 and 17. Their appearance and the fact that Schwann cell cytoplasm has degenerated favor the suggestion that they are neurites. If indeed neurites, they would not normally have been associated with myelin-containing Schwann cells. We cannot say at this time whether the processes could be axonal sprouts or regenerated or regrouped neurites. In the regeneration following Wallerian degeneration of rat dorsal root in situ, more than one axon may appear within the basement membrane encircling a Schwann cell which had previously invested only a single myelinated axon (16).

DISCUSSION

The series of events that occur in the nerve fascicles of irradiated dorsal root ganglion cultures must be considered in relation to the cytological events occurring in the culture as a whole. Prior to irradiation, the cultures contain a healthy group of neurons supporting a halo of nerve fiber bundles. During the first few days after irradiation, there is a wave of cellular degeneration throughout the culture. The cells which acutely degenerate are a portion of the satellite cells in the explant (10) and many of the Schwann cells associated with unmyelinated fibers in the nerve fascicles. The neurons, though injured, generally maintain their over-all morphological integrity. At about 1 week following irradiation, neuronal cell loss begins (10). It continues steadily but slowly, leaving many neuronal somas intact though abnormal at the end of the 14-day observation period. In the nerve fascicles, a period of minor morphological change follows the initial loss of Schwann cells. During the 2nd week postirradiation, myelin changes become pronounced. The fascicles, while retaining their general framework and much of their nerve fiber content, are filled with degenerating myelin. This myelin may be contained within Schwann cell cytoplasm or associated only with necrotic remnants of the Schwann cell. After irradiation, the cultures appear incapable of engendering any cytological response for the phagocytosis of this considerable amount of free myelin debris, perhaps because of severe damage to connective tissue elements which are the usual source of phagocytes in this culture system.

Radiation Sensitivity of Schwann Cells

When the later stages of degeneration are compared to earlier stages, it is clear that a dichotomy exists between the radiation sensitivity of cultured Schwann cells investing myelinated fibers and that of cultured Schwann cells investing unmyelinated fibers. In dorsal root ganglia irradiated in vitro, Schwann cells investing unmyelinated axons are more radiosensitive than those related to myelinated axons, on the basis of both the rapid onset of degeneration (within 24 hr) and the accelerated temporal sequence of cell death. Schwann cells investing myelinated axons appear relatively normal during the early postirradiation period, and then undergo gradual deterioration

FIGURE 8 Node of Ranvier (arrow) in a control living culture. In the bright-field photomicrograph (Fig. 8 *a*), the node measures ~3.5 μ. Observation of the same fiber in the polarizing microscope (Fig. 8 *b*) reveals that the bright refractile myelin sheath extends to essentially the same nodal position as depicted in *a*. × 690.

FIGURE 9 Abnormal node of Ranvier (arrow to arrow) in a living culture *8 days following irradiation*. The bright-field photomicrograph (Fig. 9 *a*) shows a greatly lengthened node, the distance between arrows measuring ~100 μ. Polarizing microscopy (Fig. 9 *b*) confirms that the myelin sheaths end at nearly the same nodal position as shown in *a*. × 690.

FIGURE 10 An electron micrograph of the paranodal region of a lengthened node, most of which extends beyond that shown in the figure. The terminal loops (*tl*) and internal and external regions of the myelin sheath show signs of marked deterioration. The interlacing Schwann cell projections at the nodal junction have ruptured, leaving the axon denuded. Schwann cell (*scm*) degeneration is prevalent throughout this field. *8 days after irradiation*. × 36,000.

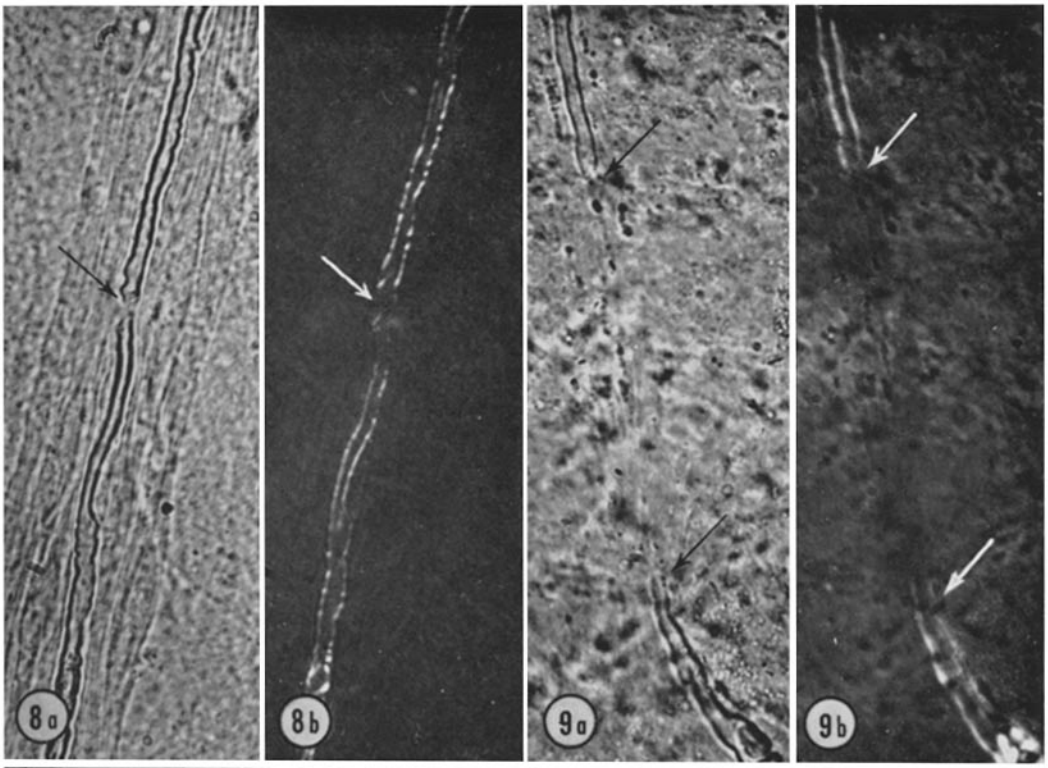
8a
8b
9a
9b

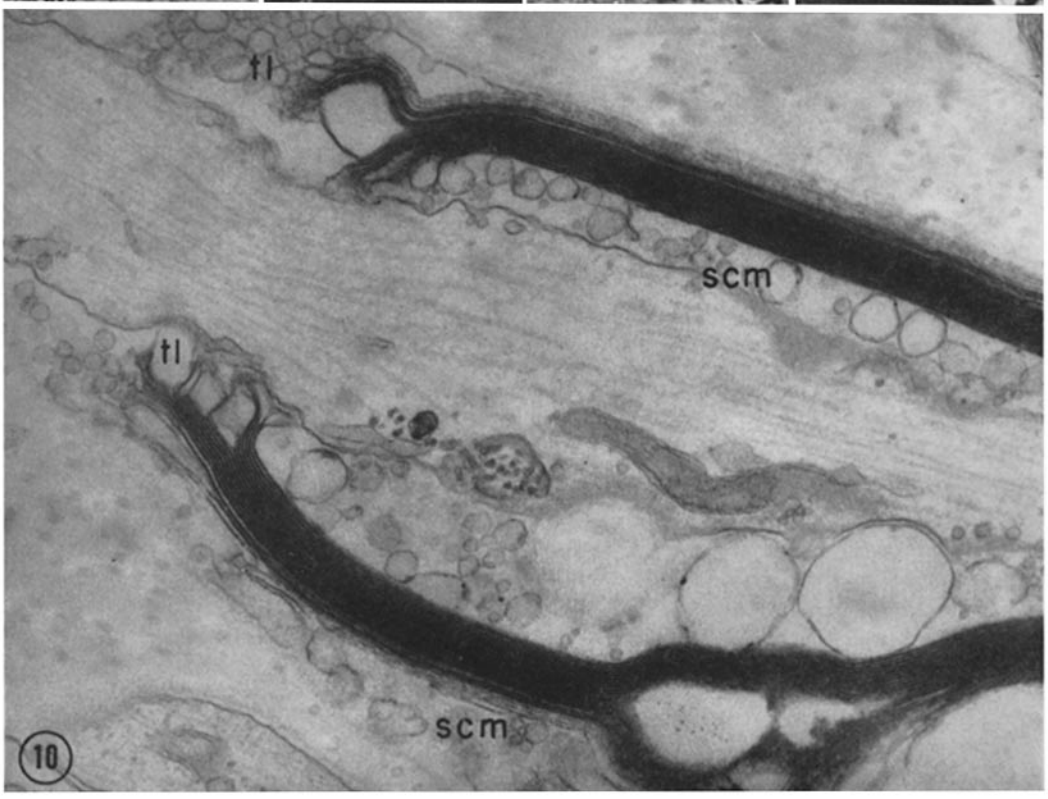
tl
scm
tl
scm
10

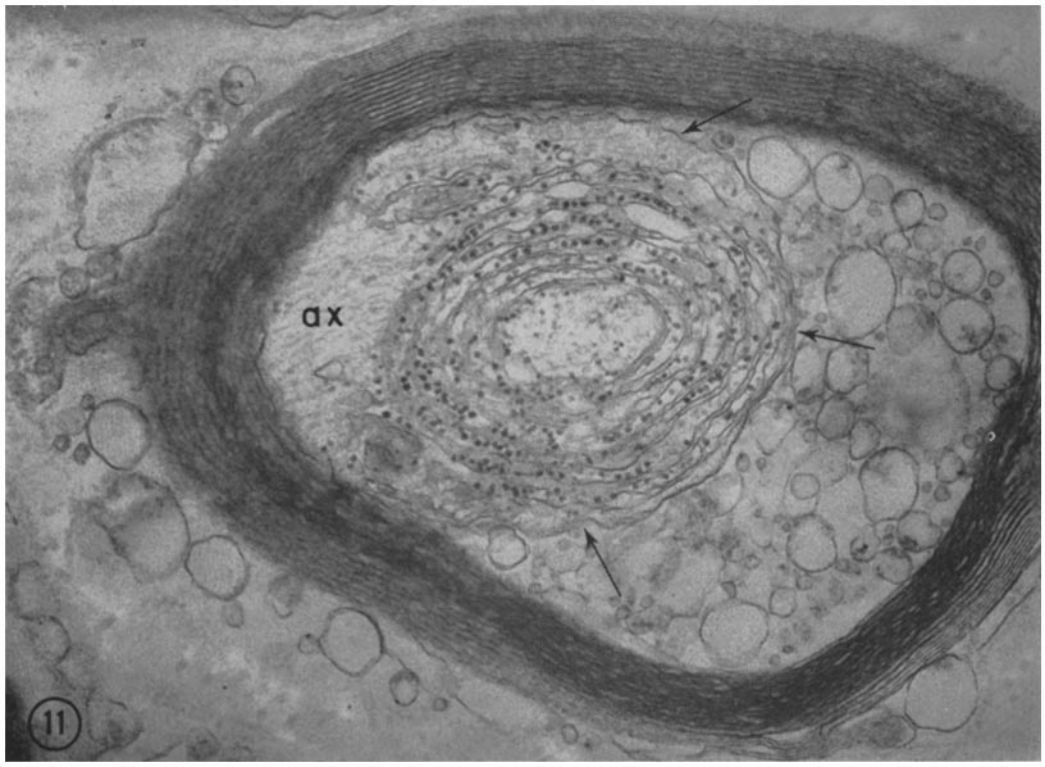

FIGURE 11 An unusual membranous array containing 330 A granules, presumed to be glycogen, within a myelinated axon (*ax* + arrows). Schwann cell and myelin breakdown is in progress. *8 days after irradiation.* × 37,000.

with time. Andres (7) did not describe differences in response of the Schwann cells associated with myelinated or unmyelinated nerve fibers during the 1st week following irradiation with 20 krad of protons in vivo. Confining his electron microscopic observations primarily to longer postirradiation periods, he did observe partial or complete denuding of unmyelinated axons; this denuding may have resulted from an earlier unnoted injury to the Schwann cells normally associated with these fibers. Thus, it appears that, except for the suggestion from the work of Isomäki et al. (5), this difference in radiation sensitivity has not been recognized in in vivo studies. The difference may suggest that the Schwann cells investing unmyelinated axons are in a more active metabolic state, maintaining several axons within a single cell, than the Schwann cells investing a single myelinated axon. Hicks (25) has pointed out that the degree of metabolic activity of cells comprising nervous tissue may be an important factor in their susceptibility, or resistance, to radiation exposure. A further suggestion that there may be metabolic differences between myelinating and nonmyelinating Schwann cells comes from the observations that unmyelinated axons appear to survive longer in the distal stump after Wallerian degeneration than do myelinated axons (reviewed in 26); the nonmyelinating Schwann cell may offer more active support for the injured fiber than does the myelinating Schwann cell. Novikoff et al. (27) have recently demonstrated histochemically that nucleoside phosphatases are present in or near unmyelinated axons and not in myelinated axons, whereas the converse is true for acetylcholinesterase localization.

Myelin Degeneration within Schwann Cells

The similarity between the onset of this intra-Schwann cell myelin degeneration in irradiated cultures and the pattern of degeneration after administration of diphtherial toxin is worthy of

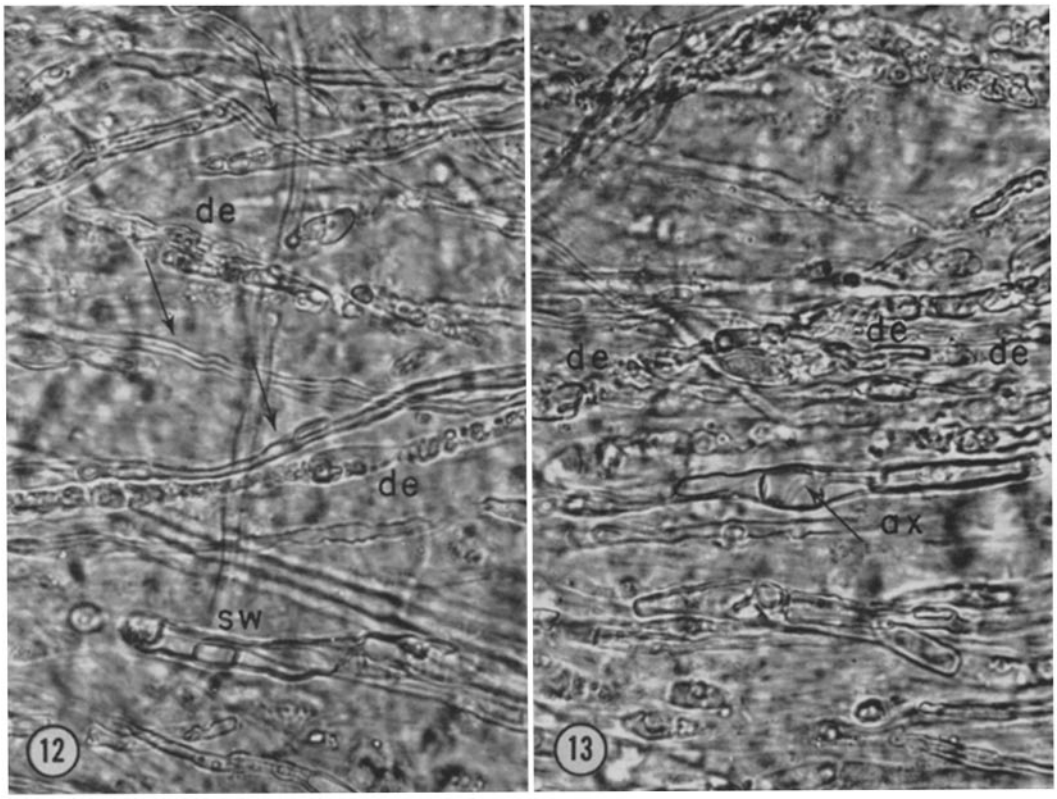

FIGURE 12 This photomicrograph of a living culture *14 days following irradiation* shows fibers undergoing Wallerian-like degeneration (*de*) or myelin swelling and distortion (*sw*). These may be compared to nearby normal-appearing fibers (arrows). × 700.

FIGURE 13 In this photomicrograph of a similar fascicle region in a living culture, myelin swelling can be seen occurring around intact, but distorted axons (*ax*—arrow). Wallerian-like degeneration (*de*) is visible in several neighboring fibers. × 700.

note. Peterson and Murray (17) have shown that myelinated spinal ganglion cultures begin to show signs of myelin damage on about the 3rd day after application of diphtherial toxin. The first sign is an increase in nodal length. This is followed by fragmentation and ovoid formation of the myelin in the affected segment, progressing from both nodes toward the centrally located Schwann nucleus. In the irradiated cultures, myelin damage is also first seen as a nodal lengthening. Thus, in both types of degeneration the node-supporting function of the Schwann cell appears to be affected first. Subsequently, the tubular form of the myelin may be replaced by a series of intracytoplasmic myelin ovoids, for some irradiated Schwann cells retain the ability to take up their myelin debris. In both diphtherial toxin–treated (17) and irradiated cultures, the axon is generally retained. In irradiated cultures, it can be seen in close association with myelin-filled Schwann cells (Fig. 5).

After the initial uptake of myelin fragments, a difference becomes evident in the digestive capacity of the Schwann cell following diphtherial toxin administration and irradiation. In diphtherial toxin–treated cultures (17), the Schwann cell retracts, pulling the fragments of myelin together. During the following weeks, digestion of these myelin fragments is completed. The diphtheritic toxin–damaged cell has, in addition, the ability to remyelinate the affected segment (17). The irradiated Schwann cell appears to digest its

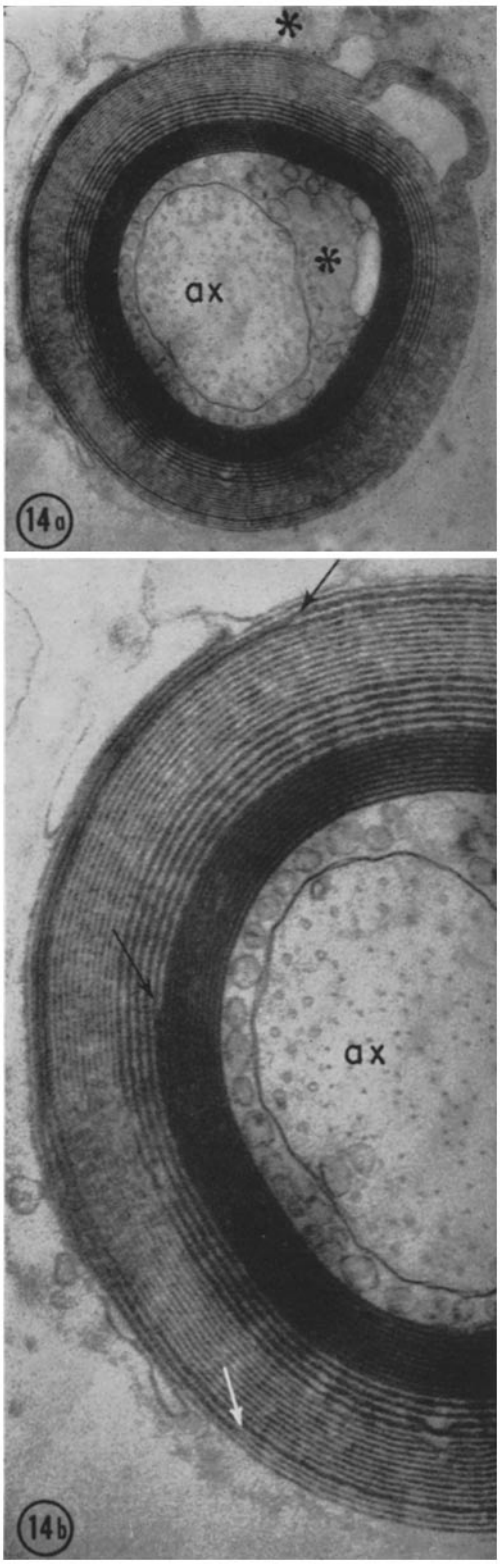

engulfed myelin more slowly than do diphtherial toxin–treated Schwann cells (or those responding to Wallerian degeneration) (17). Its appearance is not that of a cell hypertrophied for a new role of myelin digestion but that of a cell most likely unable to synthesize the required digestive proteins (enzymes) because of a decreased ribosomal content and the presence of pathological cell organelles. A number of electron microscopic in vivo studies (15, 18, 19) have reported signs of hypertrophy in Schwann cells undertaking the process of myelin digestion, particularly stressing an increase in the number of cytoplasmic ribosomes. This may be interpreted as a prelude to the protein synthesis associated with the increased number of lysosomes (20, 28) and lysosomal enzymes (20) observed during myelin digestion. It is known that, in Wallerian degeneration in vivo, myelin sheaths are physically broken up but chemically little changed during the first 10 days after nerve section (29, 30). Chemical changes in the degenerating myelin follow this initial period. It is possible that some irradiated Schwann cells have the capacity for physical breakdown of the myelin tube, but suffer an impairment in the ability to synthesize the enzymes for this chemical breakdown.

Myelin Breakdown Following Schwann Cell Degeneration

One of the most noteworthy findings of the present study is the occurrence of unusual lamellar alterations in myelin sheaths undergoing degeneration after necrosis of the related Schwann cell. Because this type of breakdown does not occur until 1 or 2 wk after exposure to radiation, and then only when the related Schwann cell has undergone extensive degeneration, it would seem reasonable to relate this phenomenon principally to Schwann cell dysfunction rather than to "primary" effects of ionizing radiation on the myelin itself. This contention would appear to be supported by a comparison of this pattern of post-

FIGURE 14 A sequence of myelin splitting is depicted in these electron micrographs of a fascicle region *14 days after irradiation*. In Fig. 14 *a*, a type of myelin alteration and reordering (Type I) seen after deterioration of the related Schwann cell (*) is illustrated. The enclosed axon (*ax*) is intact. In a higher magnification (Fig. 14 *b*), the normal-appearing sheath lamellae are seen to split at the major dense line (black arrows) and the intraperiod line (white arrow), forming a subperiod of ~150 A. *a*, × 28,000. *b*, × 52,000.

FIGURE 15 This figure shows a more advanced form of the myelin splitting and reordering depicted in Fig. 14. Irregular 120–150 A lamellar structures are further divided to form 40–60 A elements (arrows). Additional breakdown takes the form of blebs inside and outside the myelin sheath. The related Schwann cell cytoplasm appears degenerated whereas the axon (*ax*) remains intact. Within the residual basement membrane are two processes (p_1, p_2) which resemble neurites. *14 days after irradiation.* × 30,000.

irradiation myelin degeneration with patterns observed in other forms of myelin breakdown. As Finean and Woolf (31) have pointed out, the most common initial sequence in myelin breakdown is the formation of independent myelin droplets (within Schwann cell cytoplasm) in which the normal characteristics of the myelin are retained. Whereas some splitting between lamellae does occur, especially on the axonal surface of the myelin as the droplets form (32), no systematic lamellar alterations are seen. In Types I, II, and III myelin breakdown, the myelin generally does not form into droplets but retains its tubular form while its lamellar organization is dramatically altered throughout large regions of the sheath. A limited number of reports of similar systematic

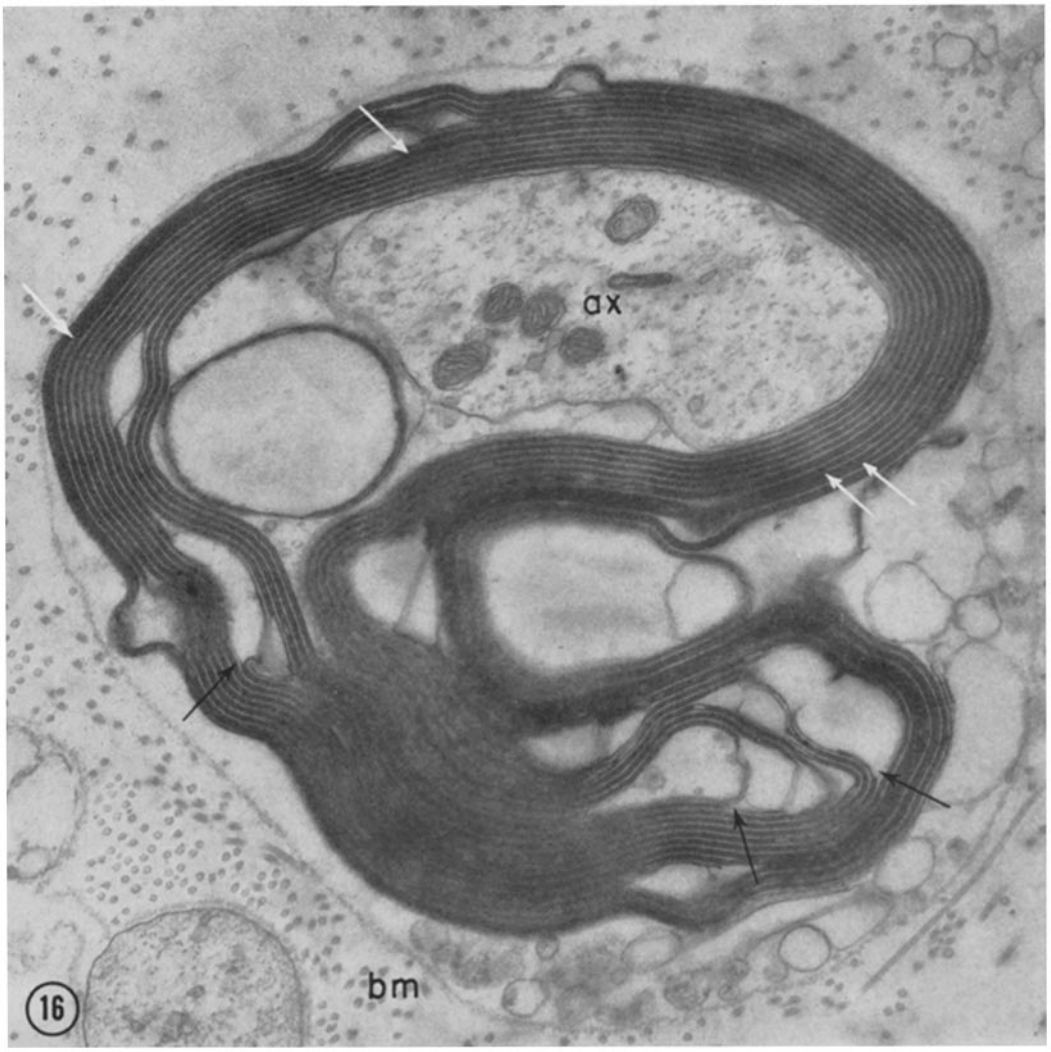

FIGURE 16 This electron micrograph illnstrates Type II myelin reordering. Dense 240 A regions of of paired lamellar elements are formed by splitting at the intraperiod line (white arrows). Further splitting and breakdown occurs within these units (black arrows). Schwann cell cytoplasm appears completely degenerated. The axon (*ax*) retains its over-all structural integrity, and the residual basement membrane (*bm*) remains generally intact. *14 days after irradiation.* × 31,000.

lamellar alterations have appeared recently: (*a*) In experimental allergic encephalomyelitis, Lampert (33, 34) has seen alterations in the more peripheral lamellae of CNS myelin as the sheath comes into contact with invading mononuclear cells; (*b*) In an experimental demyelinating lesion in spinal cord, Bunge et al. (35) have illustrated dramatic lamellar separations in CNS myelin prior to ingestion by phagocytes; and (*c*) Webster (36), has demonstrated altered lamellar patterns in PNS (peripheral nervous system) myelin in a small number of Schwann cells reacting to diphtheritic neuritis. With the exception of Webster's report, these lamellar alterations occurred in degenerating myelin that was not engulfed in cell cytoplasm. The myelin-supporting cell in both cases was believed to be undergoing acute degeneration. This might suggest that myelin lamellar alterations occurring in substantial portions of the sheath are likely to occur as a consequence of acute demise of

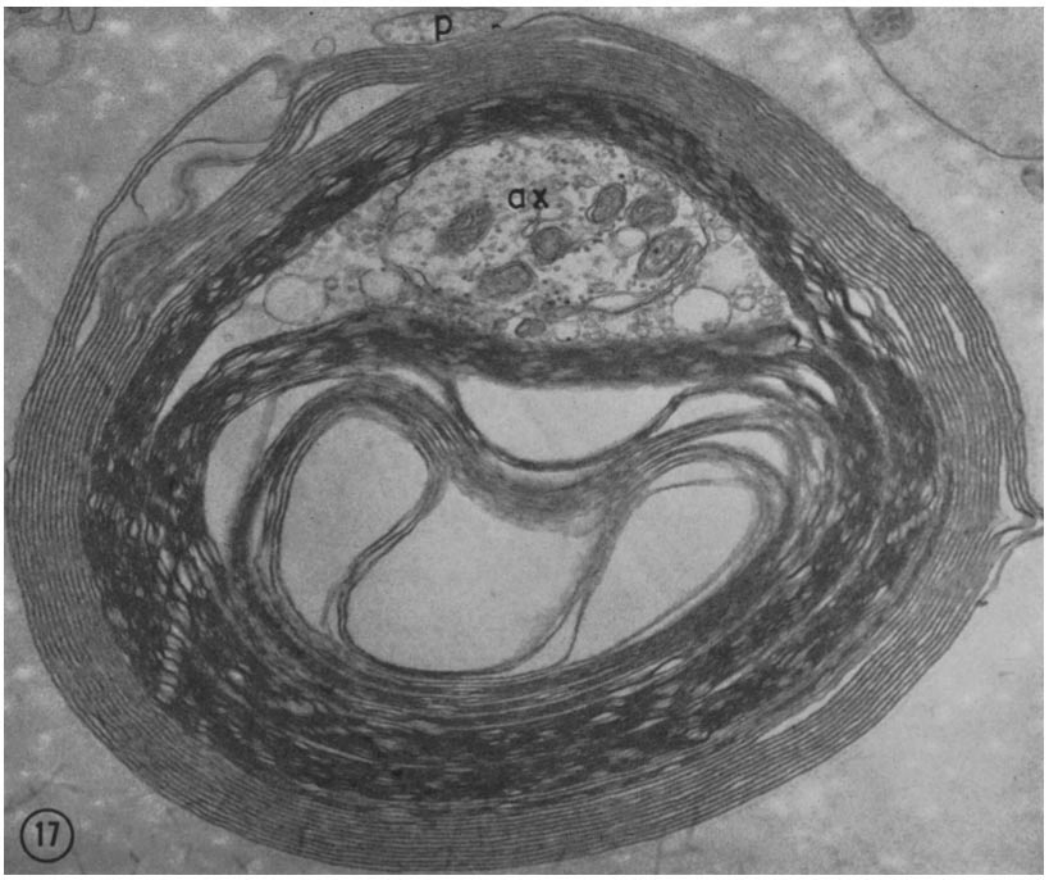

FIGURE 17 Type III myelin reordering is illustrated in this electron micrograph. The wavy 40 A inner sheath lamellar elements seem to take on a thicker (60–90 A) appearance in the peripheral regions of the sheath; here a 210–240 A spacing is formed. The axon appears between the inner sheath lamellae. A neurite-like process (*p*) is situated between the residual basement membrane of the degenerated Schwann cell and the outermost lamellar element. *14 days after irradiation.* × 31,000.

the myelin-supporting cell. To our knowledge, the present study is the only report of total degeneration of the myelin-related Schwann cell in the peripheral nervous system.

Might these observations offer significant clues toward a better definition of the metabolic contribution of the myelin-supporting cell to the maintenance of the compacted myelin layers? This question cannot be answered from the data now available but certain limited suggestions can be offered. The adhesive forces between myelin lamellae are considered to be very great (31). The regions in deteriorating sheaths following irradiation that feature a modification of lamellar structuring must involve areas in which these adhesive bonds are actively broken by physical and/or chemical forces (see especially Fernández-Morán and Finean, 37 and Adams, 43). With complete loss of function in the associated Schwann cell, abnormalities in water and/or ion content may occur in the regions of the myelin layers. This suggestion may apply particularly to the separation of myelin lamellae in the region of the intraperiod line; it is known that when myelin in isolated nerve preparations is exposed to hypotonic solutions, the state of hydration in the region of the intraperiod line increases, forcing the lamellae apart (24, 38). The resemblance between patterns produced by such hydration and Types I and II myelin degeneration after irradiation is

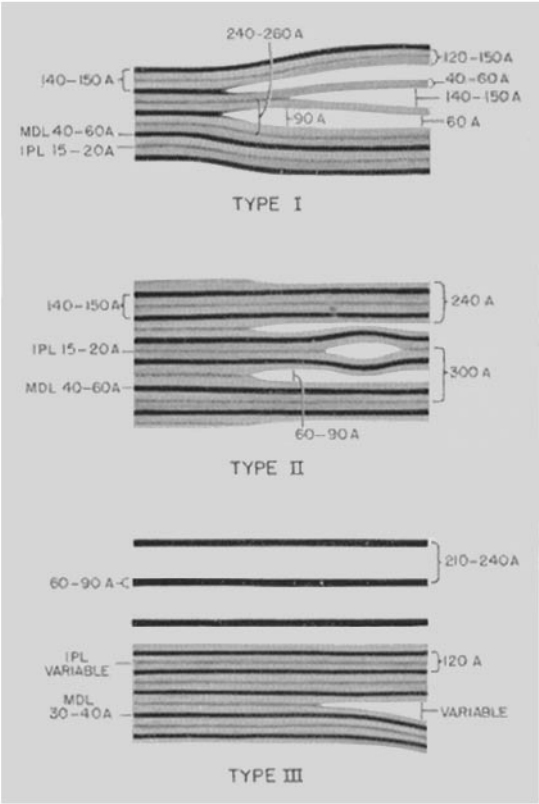

FIGURE 18 As shown in this summary diagram, Type I myelin breakdown is characterized by a 240–260 A periodic structure formed by splitting at the major dense line; a subperiod of ~150 A is produced by further splitting at the intraperiod line. Type II myelin configurations are of quite a different nature from Type I, being composed of 240 A paired lamellar elements formed by splitting in the region of every other intraperiod line. Type III appears to be unrelated to either Type I or II with its abnormal, wavy inner sheath lamellar structuring which opens out into a 210–240 A spacing.

noteworthy. Taken together, might these observations suggest that one of the normal ongoing activities of the Schwann cell is to maintain a proper state of hydration of the myelin lamellae? In CNS white matter of subjects suffering from triethyl tin-induced edema, there is a striking accumulation of fluids between myelin lamellae, with attendant separation at the intraperiod line as intramyelinic vacuoles form (39, 40). Might this suggest that in CNS myelin, too, the myelin-related cell, the oligodendrocyte, functions to constantly adjust the state of myelin hydration, triethyl tin being a specific poison for that function?

It should be pointed out that the absence of a functioning Schwann cell may contribute in other ways to the breakdown of the sheath. An abnormal physicochemical environment may be created by the release of hydrolytic enzymes from the degenerating Schwann cell cytoplasm. Such enzymes may weaken the adhesive bonds of the myelin lamellae at both the major dense and intraperiod lines. Certain hydrolytic enzymes are known to be capable of causing the breakdown of myelin in CNS disorders. Thompson (41) has suggested that cycles of degradation may develop in demyelinating diseases of the CNS whereby damage to the myelin membrane is followed by alterations in intracellular organelles (i.e., lysosomes) and release of phospholipases. Products of phospholipase activity such as lysolecithin may in turn cause further damage to the myelin. Hydrolytic enzymes have recently been demonstrated by Holtzman and Novikoff (20) to be associated with myelin undergoing breakdown during Wallerian degeneration of peripheral nerve. The formation of foamlike, reticulated structures from myelin remnants appears to be the terminal pathway of myelin degradation in this culture system. The plastic nature of these myelin blebs, the variation in the thickness of their outlines, and the seemingly empty or fluid nature of their contents suggest that degradation of protein and lipid components alike may be taking place in these regions.

Primary (Direct) Versus Secondary (Indirect) Effects of Irradiation

This study details the sequence of cytological changes which occur in organotypic nerve fiber bundles irradiated in vitro. These changes are, therefore, independent of secondary effects attributable to a radiation-damaged vascular supply or other host-associated humoral or inflammatory responses. The resultant pathology bears many points of similarity to peripheral nerve irradiated in vivo. As mentioned under Observations, the present study confirms the relative resistance of the axon to ionizing radiation. Andres (7) demonstrated this in his electron microscopic study of peripheral nerve irradiated in vivo. Goldring (42) had previously noted the greater radiosensitivity of "sheath cells" vs. axonal

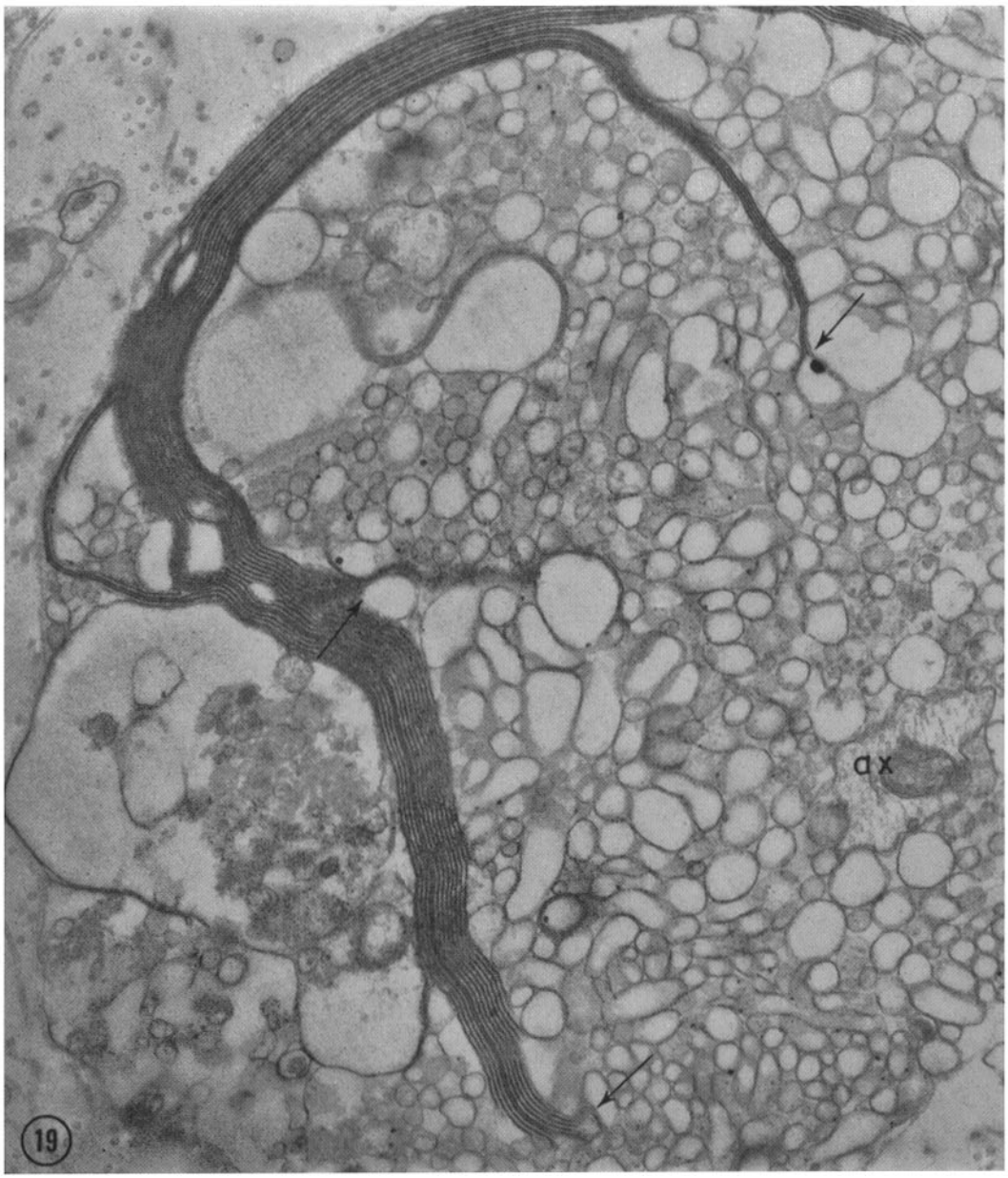

FIGURE 19 This electron micrograph illustrates a common form of terminal myelin degeneration associated with nerve fibers completely devoid of viable Schwann cell cytoplasm. Blebbing of myelin elements occurs principally at the exposed lamellar endings (arrows). A distorted axon (*ax*) may be seen among the myelin blebs contained within the residual basement membrane of the defunct Schwann cell. *14 days after irradiation.* × 30,000.

processes in avian dorsal root ganglia X-irradiated in ovo and in vitro. The present study demonstrates that, among these "sheath cells," the Schwann cells are particularly radiosensitive and that there is a differential sensitivity between Schwann cells associated with unmyelinated fibers and those associated with myelinated fibers. Whether this observation has an in vivo correlate

cannot be completely assessed until further work is available on comparable in vivo material during the same early period after irradiation. The work of Isomäki et al. (5) in the frog strongly suggests that a similar differential radiation response may be elicited in vivo. Axonal accumulations of glycogen have been observed in the present study as well as in axons of frog sympathetic neurons irradiated in vivo (23). The persistence of the endoneurial basement membrane after the demise of the related Schwann cell noted in this study has also been observed after irradiation in vivo (7). Myelin damage is common to both this in vitro and comparable in vivo systems (see Introduction). It, appears, therefore that these manifestations of radiation exposure may result from "direct" effects of ionizing radiations on the fascicle elements themselves.

In addition to establishing this important point concerning radiation cytopathology in peripheral nerve fascicles, the present study has revealed unusual alterations in the structure of the myelin sheath not heretofore reported as a postirradiation change. In the progression of myelin changes observed, neither intervention of macrophages nor proliferation of Schwann cells from nearby unirradiated regions occurs, factors undoubtedly contributing to the unusual patterns of myelin breakdown. This organotypic in vitro system has made possible the study of these myelin changes through their final degenerative stages uncomplicated by ancillary inflammatory, circulatory, and humoral host-associated reactions. These observations on irradiated ganglion cultures should provide a useful basis for future evaluation of the cytopathological effects of ionizing radiations on mammalian peripheral nerve in vivo.

This research was conducted while the senior author was a Postdoctoral Fellow of the National Institutes of Neurological Diseases and Blindness (Grant No. 5T1-NB 5242 administered by Dr. M. B. Carpenter). The study was supported by National Institutes of Health Grant NB 04235 and National Multiple Sclerosis Society Grant 328 to Dr. R. P. Bunge, and National Institutes of Health Grant 5T1-GM-256-04 to Dr. W. M. Copenhaver.

We gratefully acknowledge the assistance of Dr. Roberts Rugh and the Radiological Research Laboratory, Columbia University, in the use of the X-ray facility and in determining dosimetry. The valuable assistance of Mr. Philip Chang and Mr. Vincent Blancuzzi in handling the cultured material is sincerely appreciated.

Portions of the material in this paper have been reported at the American Association of Anatomists, 1965 (*Anat. Record.* 1965, **151:** 382) and at the 8th International Congress of Neurology, 1965 (*Excerpta Med., Internat. Congr. Ser. 94.* 1965. E219).

Received for publication 27 July 1966.

REFERENCES

1. REDFIELD, E. S., A. C. REDFIELD, and A. FORBES. 1922. The action of beta rays of radium on excitability and conduction in the nerve trunk. *Am. J. Physiol.* **59:** 203.
2. LEBOUCQ, G. 1934. Action des rayons X sur la formation de la myéline chez le rat blanc. *Rev. Belge. Sci. Méd.* **6:** 383.
3. MOGIL'NITSKIY, B. N., L. D. PODLYASHCHUK, and M. T. SANTOTSKIY. 1936. The effects of X-rays on the peripheral (somatic and sympathetic) nervous system. *Sb. Trudov. Po. Rentgenol.* **2:** 147.
4. JANZEN, A., and S. WARREN. 1942. Effects of roentgen rays on the peripheral nerve of the rat. *Radiology.* **38:** 333.
5. ISOMÄKI, A. M., R. M. BERGSTRÖM, and E. KIVALO. 1962. Ultrastructural changes in the sensory nerve fibers in the skin of the frog (*Rana temporaria*) after circumscript irradiation with Po^{210} α-particles (5.3 MeV). *Acta Pathol. Microbiol. Scand.* **54:** 190.
6. BERGSTRÖM, R. 1962. Changes in peripheral nerve tissue after irradiation with high energy protons. *Acta Radiol.* **58:** 301.
7. ANDRES, K. H. 1963. Elektronmikroscopische Untersuchungen über strukturveränderungen an den Nervenfasern in Rattenspinalganglien nach Bestrahlung mit 185 Mev-Protonen. *Z. Zellforsch. mikroskop. Anat.* **61:** 1.
8. BUNGE, M. B., R. P. BUNGE, E. R. PETERSON, and M. R. MURRAY. 1967. A light and electron microscope study of long-term organized cultures of rat dorsal root ganglia. *J. Cell Biol.* **32:** 439.
9. BUNGE, M. B., R. P. BUNGE, and E. R. PETERSON. 1965. An electron microscope study of cultured rat spinal cord. *J. Cell Biol.* **24:** 163.
10. MASUROVSKY, E. B., M. B. BUNGE, and R. P. BUNGE. 1967. Cytological studies of organotypic cultures of rat dorsal root ganglia following X-irradiation *in vitro*. I. Changes in neurons and satellite cells. *J. Cell. Biol.* **32:** 467.
11. ZEMAN, W., H. J. CURTIS, and C. P. BAKER. 1961. Histopathologic effect of high-energy-particle

microbeams on the visual cortex of the mouse brain. *Radiation Res.* **15:** 496.

12. HAYMAKER, W. 1962. Morphological changes in the nervous system following exposure to ionizing radiation. *In* Effects of Ionizing Radiation on the Nervous System, Proceedings Symposium, Vienna, 1961. International Atomic Energy Agency, Vienna, 309.
13. BROWNSON, R. H., M. A. SUTER, and D. A. DILLER. 1963. Acute brain damage induced by low dosage X-irradiation. *Neurology.* **13:** 181.
14. THOMAS, P. K. 1964. Changes in the endoneurial sheaths of peripheral myelinated nerve fibers during Wallerian degeneration. *J. Anat. (London).* **98:** 175.
15. NATHANIEL, E. J. H., and D. C. PEASE. 1963. Degenerative changes in rat dorsal roots during Wallerian degeneration. *J. Ultrastruct. Res.* **9:** 511.
16. NATHANIEL, E. J. H., and D. C. PEASE. 1963. Regenerative changes in rat dorsal roots following Wallerian degeneration. *J. Ultrastruct. Res.* **9:** 533.
17. PETERSON, E. R., and M. R. MURRAY. 1965. Patterns of peripheral demyelination *in vitro*. *Ann. N. Y. Acad. Sci.* **122:** 39.
18. SATINSKY, D., F. A. PEPE, and C. N. LIU. 1964. The neurilemma cell in peripheral nerve degeneration and regeneration. *Exptl. Neurol.* **9:** 441.
19. BLÜMCKE, S., and H. R. NIEDORF. 1966. Electron microscope studies of Schwann cells during the Wallerian degeneration with special reference to the cytoplasmic filaments. *Acta Neurol.* **6:** 46.
20. HOLTZMAN, E., and A. B. NOVIKOFF. 1965. Lysosomes in the rat sciatic nerve following crush. *J. Cell Biol.* **27:** 651.
21. WEBSTER, H., DE F., D. SPIRO, B. WAKSMAN, and R. D. ADAMS. 1961. Phase and electron microscopic studies of experimental demyelination. II. Schwann cell changes in guinea pig sciatic nerves during experimental diphtheritic neuritis. *J. Neuropathol. and Exptl. Neurol.* **20: 5.**
22. STEINER, J. W., M. KATSUMI, and M. J. PHILLIPS. 1964. Electron microscopy of membrane-particle arrays in liver cells of ethionine-intoxicated rats. *Am. J. Pathol.* **44:** 169.
23. PICK, J. 1965. The fine structure of sympathetic neurons in X-irradiated frogs. *J. Cell Biol.* **26:** 335.
24. FINEAN, J. B., and R. E. BURGE. The determination of the Fourier transform of the myelin layer from a study of swelling phenomena. *J. Mol. Biol.* **7:** 672.
25. HICKS, S. P. 1953. Developmental brain metabolism. Effects of cortisone, anoxia, fluoroacetate, radiation, insulin, and other inhibitors on the embryo, newborn and adult. *Arch. Pathol.* **55:** 302.
26. LEE, J. C.-Y. 1963. Electron microscopy of Wallerian degeneration. *J. Comp. Neurol.* **120:** 65.
27. NOVIKOFF, A. B., N. QUINTANA, H. VILLAVERDE, and R. FORSCHIRM. 1966. Nucleoside phosphatase and cholinesterase activities in dorsal root ganglia and peripheral nerve. *J. Cell Biol.* **29:** 525.
28. WELLER, R. O. 1965. Diphtheritic neuropathy in the chicken: An electron microscopic study. *J. Pathol. and Bacteriol.* **89:** 591.
29. NOBACK, C. R., AND J. A. REILLY. 1956. Myelin sheath during degeneration and regeneration. II. Histochemistry. *J. Comp. Neurol.* **105:** 333.
30. JOHNSON, A. O., A. R. MCNABB, and R. ROSSITER. 1950. Chemistry of Wallerian degeneration. *Arch. Neurol. and Psychiat.* **64:** 105.
31. FINEAN, J. B., AND A. L. WOOLF. 1962. An electron microscope study of degenerative changes in human cutaneous nerve. *J. Neuropathol. and Exptl. Neurol.* **21:** 105.
32. WEBSTER, H. DE F. 1962. Experimental diphtheritic neuritis and Wallerian degeneration; a comparative study of demyelination utilizing phase and electron microscopy. *In Proc. 4th Internat. Congr. Neuropathol.* **2:** 6.
33. LAMPERT, P., and S. CARPENTER. 1965. Electron microscopic studies on the vascular permeability and the mechanism of demyelination in experimental allergic encephalomyelitis. *J. Neuropathol. and Exptl. Neurol.* **11:** 24.
34. LAMPERT, P. 1965. Demyelination and remyelination in experimental allergic encephalomyelitis. *Neuropathol. and Exptl. Neurol.* **24:** 371.
35. BUNGE, M. B., R. P. BUNGE, and H. RIS. 1961. Ultrastructural study of remyelination in an experimental lesion in adult cat spinal cord. *J. Biophys. Biochem. Cytol.* **10:** 67.
36. WEBSTER, H. DE F. 1964. Some ultrastructural features of segmental demyelination and myelin regeneration in peripheral nerve. *In* Progress in Brain Research. Mechanisms of Neural Regeneration. M. Singer and J. P. Schadé, editors. Elsevier Publishing Co., Amsterdam. **13:** 151.
37. FERNÁNDEZ-MORÁN, H., and J. B. FINEAN. 1957. Electron microscope and low-angle X-ray diffraction studies of the nerve myelin sheath. *J. Biophys. Biochem. Cytol.* **3:** 725.
38. ROBERTSON, J. D. 1958. Structural alterations in nerve fibers produced by hypotonic and hypertonic solutions. *J. Biophys. Biochem. Cytol.* **4:** 349.

39. ALEU, F. P., R. KATZMAN, and R. D. TERRY. 1963. Fine structure and electrolyte analysis of cerebral edema induced by alkyl tin intoxication. *J. Neuropathol. and Exptl. Neurol.* **22:** 403.

40. SCHEINBERG, L. J. TAYLOR, F. HERZOG, and S. MANDELL. 1966. Optic and peripheral nerve response to triethyl tin intoxication in the rabbit: biochemical and ultrastructural studies. *J. Neuropathol. and Exptl. Neurol.* **25:** 202.

41. THOMPSON, R. H. S. 1964. Lipolytic enzymes and demyelination. *In* Metabolism and Physiological Significance of Lipids. R. M. C. Dawson and D. N. Rhodes, editors. John Wiley and Sons, Ltd., London. 541.

42. GOLDRING, I. P. 1956. The effects of X-rays on growth of spinal ganglia from 6-and 12-day chick embryos in tissue culture. *Radiation Res.* **5: 390.**

43. ADAMS, C. W. M., M. Z. M. IBRAHIM, and S. LEIBOWITZ. 1965. Demyelination. *In* Neurohistochemistry. C. W. M. Adams, editor. Elsevier Publishing Company, Amsterdam. Chap. 11.